

## Supporting Information

### Effects of Ag Nanoparticle Coated Metal Electrodes on Electrochemical CO<sub>2</sub>

#### Reduction in Aqueous KHCO<sub>3</sub>

Kayo KOIKE<sup>a</sup>, Miyuki NARA<sup>a</sup>, Minori FUKUSHIMA<sup>a</sup>, Hyojung BAE<sup>b</sup>, Jun-Seok HA<sup>b</sup>, Katsushi FUJII<sup>a,\*</sup>,§, and Satoshi WADA<sup>a</sup>

<sup>a</sup>*Photonics Control Technology Team, RIKEN Center for Advanced Photonics, 2-1 Hirosawa, Wako, Saitama 351-0198 Japan*

<sup>b</sup>*Optoelectronics Convergence Research Center, Chonnam National University, 77 Yongbong-ro, Buk-gu, Gwangju 61186, Republic of Korea*

\* Corresponding Author: [katsushi.fujii@riken.jp](mailto:katsushi.fujii@riken.jp)

§ ECSJ Active Member

#### CONTENTS

- Time-dependent potentials (vs. Ag/AgCl (3 mol/dm<sup>3</sup> NaCl aqueous solution)) and faradaic efficiencies (FEs) of gas products and liquid products.
- Cyclic voltammograms of pure metals (four cycles).
- Cyclic voltammograms of Ag-nanoparticle spray-coated metals (four cycles).

The areas of the Ag, Cu, Sn, Ti, and Zn cathodes were 5.18 cm<sup>2</sup> and that for Au was 4.51 cm<sup>2</sup>.

**S1. Time-dependent potentials (vs. Ag/AgCl (3 mol/dm<sup>3</sup> NaCl aqueous solution)) and faradaic efficiencies (FEs) of the gas products and selected liquid products**

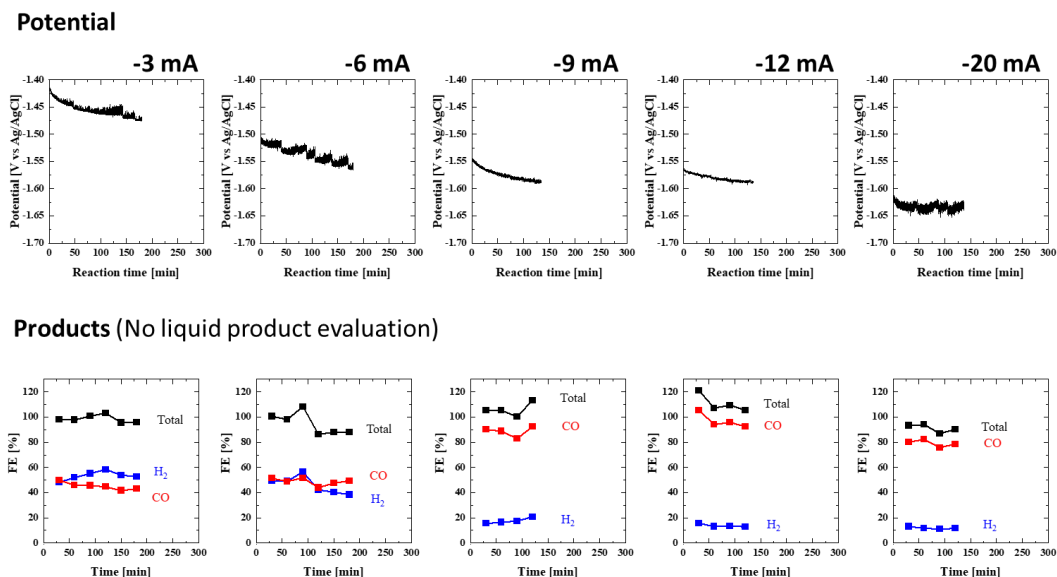


Fig. S1-1 Time-dependent potentials (vs. Ag/AgCl (3 mol/dm<sup>3</sup> NaCl aqueous solution)) and faradaic efficiencies (FEs) of the gas products for the Ag electrode at applied currents of (from left to right)  $-3$ ,  $-6$ ,  $-9$ ,  $-12$ , and  $-20$  mA.

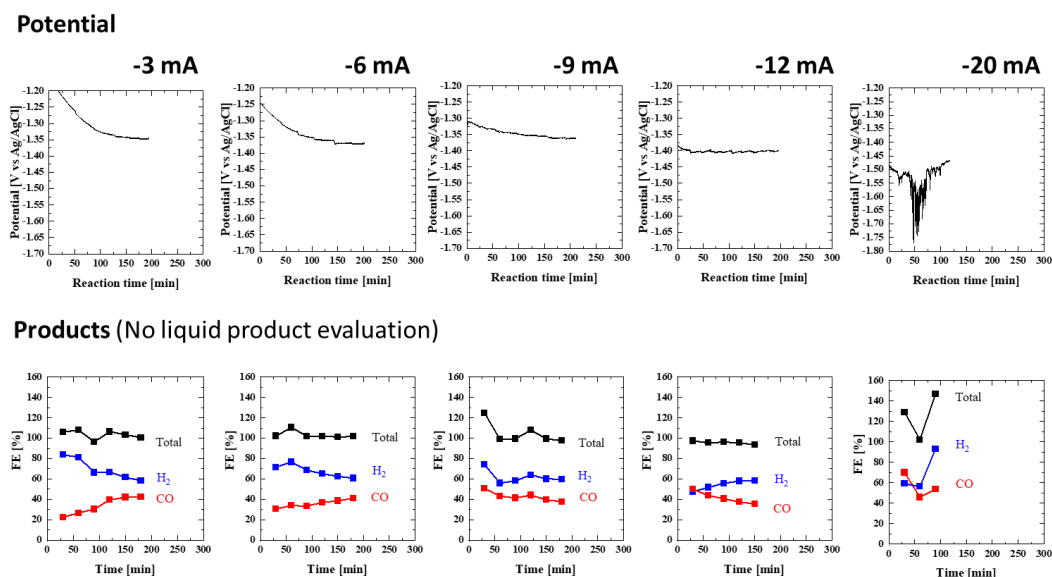
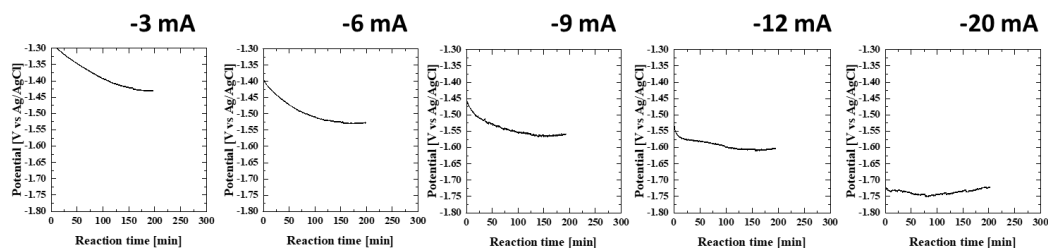


Fig. S1-2 Time-dependent potentials (vs. Ag/AgCl (3 mol/dm<sup>3</sup> NaCl aqueous solution)) and faradaic efficiencies (FEs) of the gas products for the Au electrode at applied currents of (from left to right)  $-3$ ,  $-6$ ,  $-9$ ,  $-12$ , and  $-20$  mA.

### Potential



### Products (with liquid products evaluation)

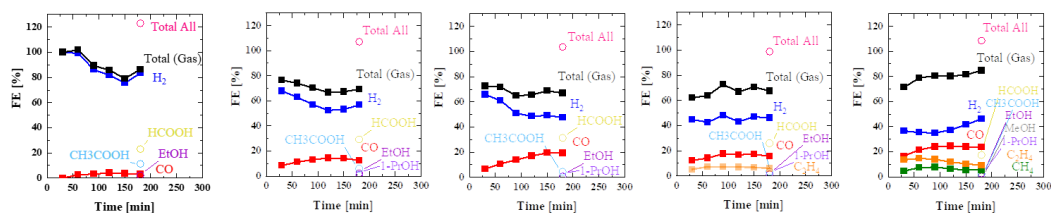
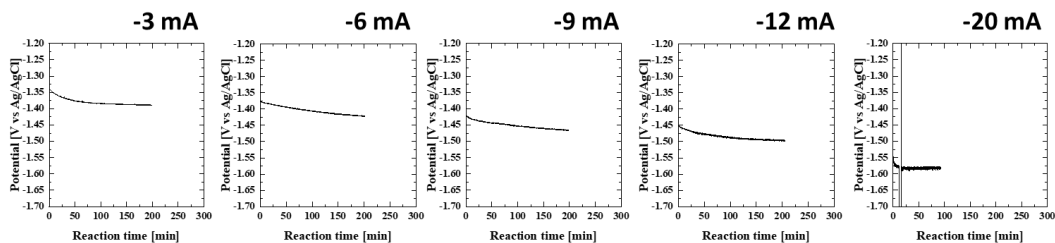


Fig. S1-3 Time-dependent potentials (vs. Ag/AgCl (3 mol/dm<sup>3</sup> NaCl aqueous solution)) and faradaic efficiencies (FEs) of the gas products for the Cu electrode at applied currents (from left to right) of -3, -6, -9, -12, and -20 mA. The liquid products in the electrolytes were evaluated after reaction.

### Potential



### Products (Liquid product evaluation was only performed for -20 mA sample)

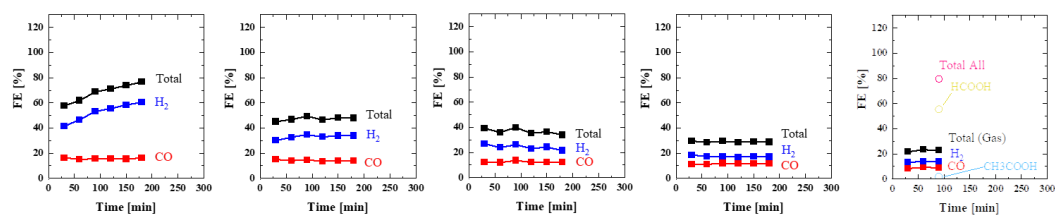
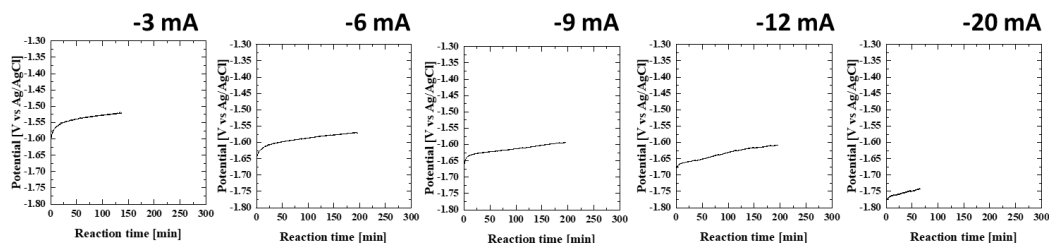


Fig. S1-4 Time-dependent potentials (vs. Ag/AgCl (3 mol/dm<sup>3</sup> NaCl aqueous solution)) and faradaic efficiencies (FEs) of the gas products for the Sn electrode at applied currents of (from left to right) -3, -6, -9, -12, and -20 mA. The liquid products produced in the electrolytes at -20 mA were evaluated after the reaction. “Total All” indicates the sum of gas and liquid products.

### Potential



### Products (No liquid product evaluation)

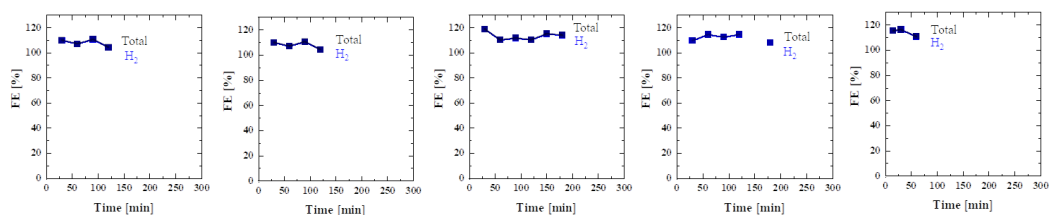
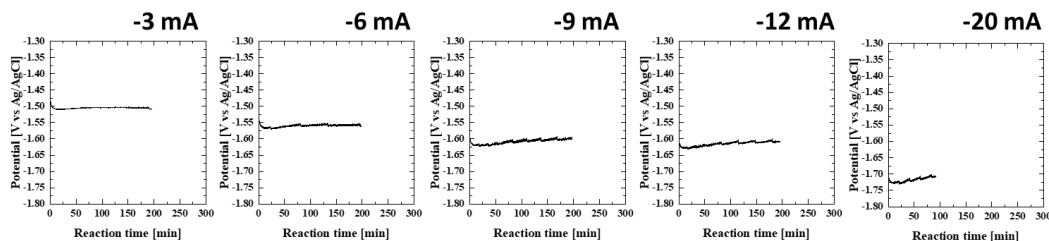


Fig. S1-5 Time-dependent potentials (vs. Ag/AgCl (3 mol/dm<sup>3</sup> NaCl aqueous solution)) and faradaic efficiencies (FEs) of gas products for the Ti electrode at applied currents of (from left to right) -3, -6, -9, -12, and -20 mA.

### Potential



### Products (with liquid products evaluation)

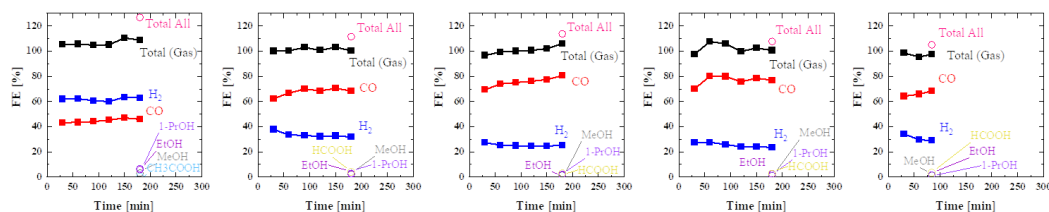
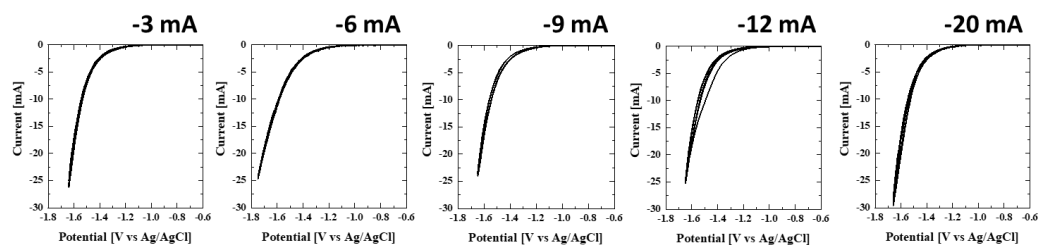


Fig. S1-6 Time-dependent potentials (vs. Ag/AgCl (3 mol/dm<sup>3</sup> NaCl aqueous solution)) and faradaic efficiencies (FEs) of gas products for the Zn electrode at applied currents of (from left to right) -3, -6, -9, -12, and -20 mA. The liquid products produced in the electrolytes were evaluated after reaction. “Total All” indicates the sum of gas and liquid products.

## S2. Cyclic voltammograms of pure metals

Before reaction



After reaction

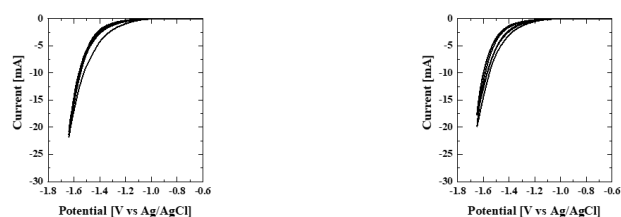
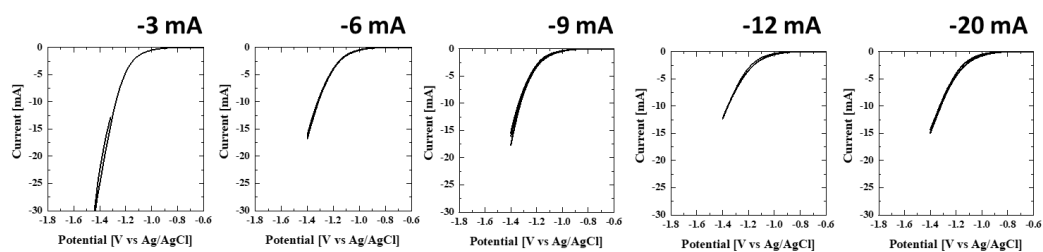


Fig. S2-1 Cyclic voltammograms (four cycles) of the Ag electrode before and after the  $\text{CO}_2$  reduction reaction.

Before reaction



After reaction

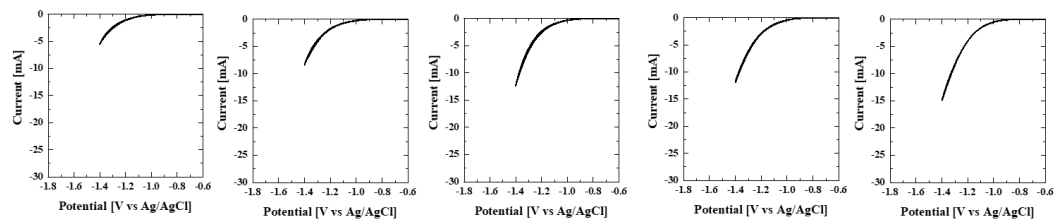
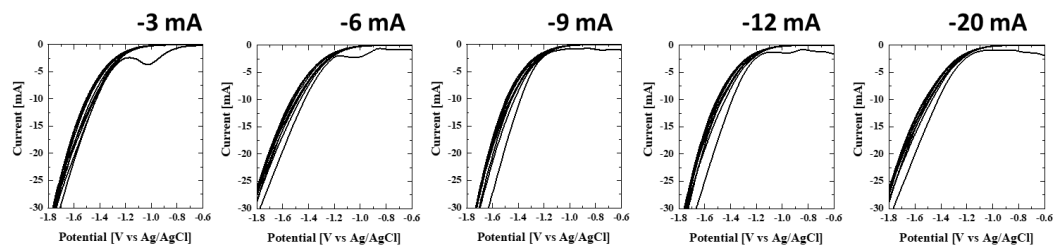


Fig. S2-2 Cyclic voltammograms (four cycles) of the Au electrode before and after the  $\text{CO}_2$  reduction reaction.

**Before reaction**



**After reaction**

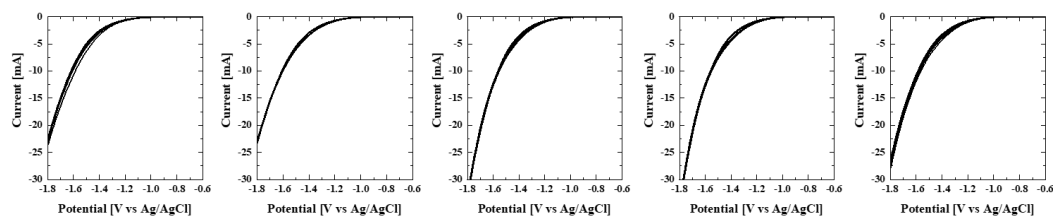
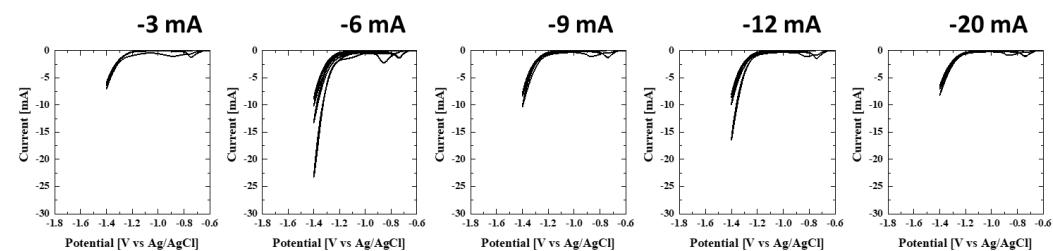


Fig. S2-3 Cyclic voltammograms (four cycles) of the Cu electrode before and after the CO<sub>2</sub> reduction reaction.

**Before reaction**



**After reaction**

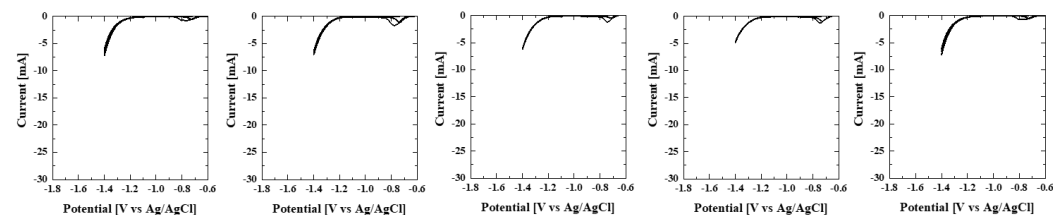
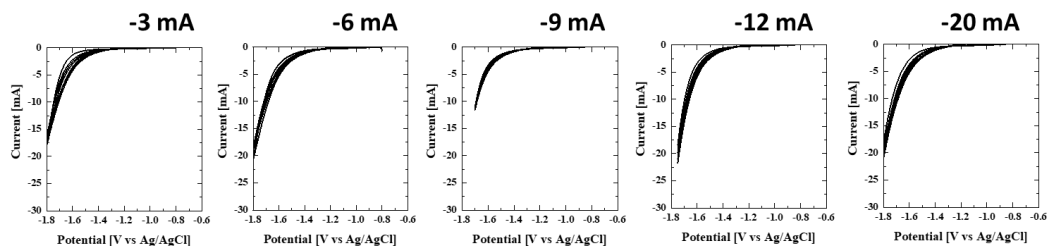


Fig. S2-4 Cyclic voltammograms (four cycles) of the Sn electrode before and after the CO<sub>2</sub> reduction reaction.

**Before reaction**



**After reaction**

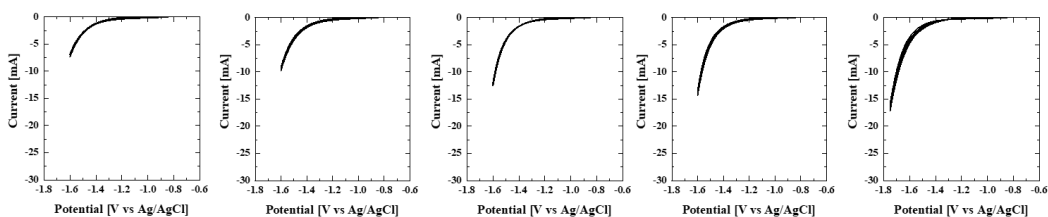
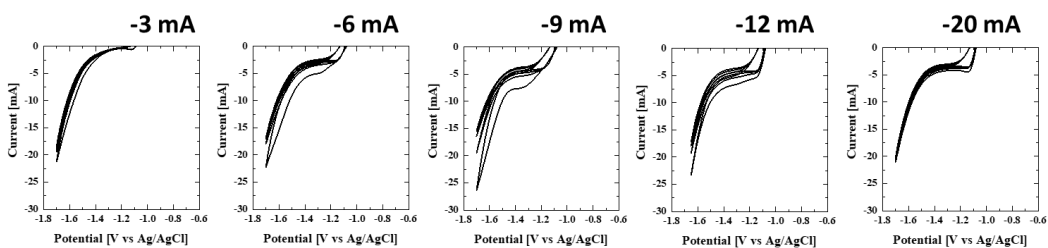


Fig. S2-5 Cyclic voltammograms (four cycles) of the Ti electrode before and after the CO<sub>2</sub> reduction reaction.

**Before reaction**



**After reaction**

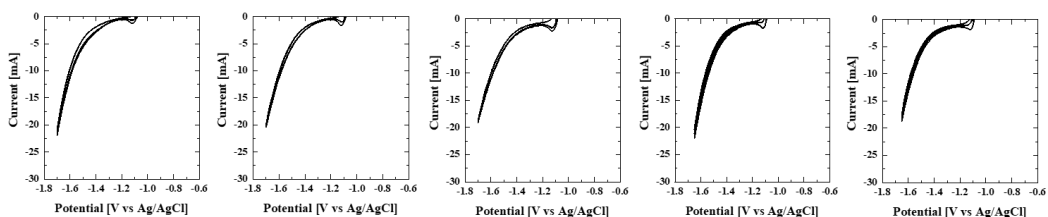


Fig. S2-6 Cyclic voltammograms (four cycles) of the Zn electrode before and after the CO<sub>2</sub> reduction reaction.

### S3. Cyclic voltammograms of Ag-nanoparticle spray-coated metals

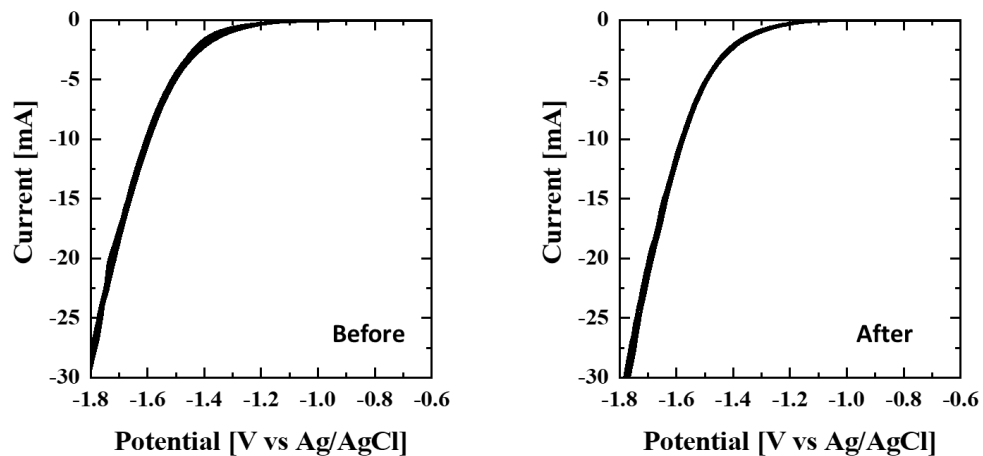


Fig. S3-1 Cyclic voltammograms four cycles) of the Ag-nanoparticle spray-coated Ag electrode before and after the CO<sub>2</sub> reduction reaction.

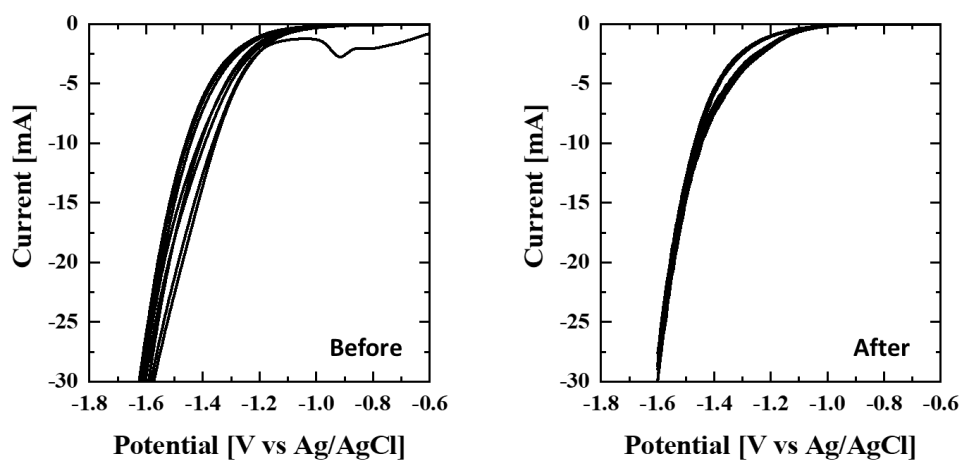


Fig. S3-2 Cyclic voltammograms four cycles) of the Ag-nanoparticle spray-coated Cu electrode before and after the CO<sub>2</sub> reduction reaction.



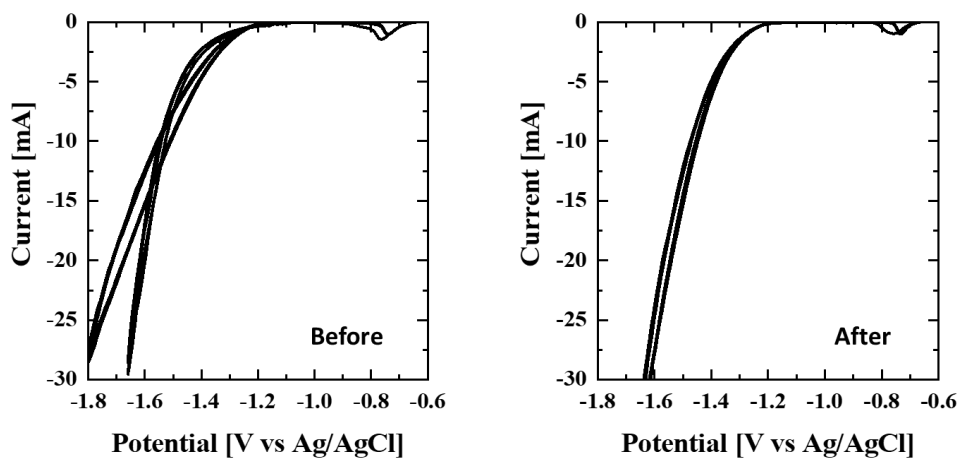


Fig. S3-3 Cyclic voltammograms (four cycles) of the Ag-nanoparticle spray-coated Sn electrode before and after the CO<sub>2</sub> reduction reaction.

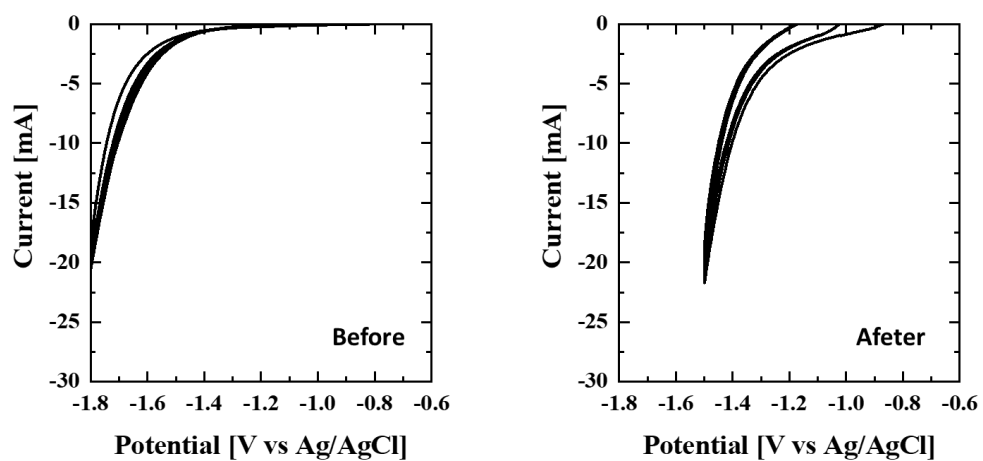


Fig. S3-4 Cyclic voltammograms (four cycles) of the Ag-nanoparticle spray-coated Ti electrode before and after the CO<sub>2</sub> reduction reaction.